



A global monthly land surface air temperature analysis for 1948–present

Yun Fan^{1,2} and Huug van den Dool¹

Received 29 January 2007; revised 16 August 2007; accepted 24 September 2007; published 12 January 2008.

[1] A station observation-based global land monthly mean surface air temperature dataset at 0.5×0.5 latitude-longitude resolution for the period from 1948 to the present was developed recently at the Climate Prediction Center, National Centers for Environmental Prediction. This data set is different from some existing surface air temperature data sets in: (1) using a combination of two large individual data sets of station observations collected from the Global Historical Climatology Network version 2 and the Climate Anomaly Monitoring System (GHCN + CAMS), so it can be regularly updated in near real time with plenty of stations and (2) some unique interpolation methods, such as the anomaly interpolation approach with spatially-temporally varying temperature lapse rates derived from the observation-based Reanalysis for topographic adjustment. When compared with several existing observation-based land surface air temperature data sets, the preliminary results show that the quality of this new GHCN + CAMS land surface air temperature analysis is reasonably good and the new data set can capture most common temporal-spatial features in the observed climatology and anomaly fields over both regional and global domains. The study also reveals that there are clear biases between the observed surface air temperature and the existing Reanalysis data sets, and they vary in space and seasons. Therefore the Reanalysis 2 m temperature data sets may not be suitable for model forcing and validation. The GHCN + CAMS data set will be mainly used as one of land surface meteorological forcing inputs to derive other land surface variables, such as soil moisture, evaporation, surface runoff, snow accumulation and snow melt, etc. As a byproduct, this monthly mean surface air temperature data set can also be applied to monitor surface air temperature variations over global land routinely or to verify the performance of model simulation and prediction.

Citation: Fan, Y., and H. van den Dool (2008), A global monthly land surface air temperature analysis for 1948–present, *J. Geophys. Res.*, 113, D01103, doi:10.1029/2007JD008470.

1. Introduction

[2] Soil hydrology models of the sort described by *Huang et al.* [1996, hereinafter referred to as H96] need, among other variables, monthly mean surface air temperature (MMSAT) as input. The original H96 model (US only) and its extension to the whole world [*Fan and van den Dool*, 2004] use temperature but only in the evaporation calculation. While temperature is thus an important input parameter, the sensitivity of evaporation, and ultimately soil moisture, to errors in temperature is not dramatic, so the MMSAT from the 344 US Climate Divisions and the Global Climate Data Assimilation System (CDAS)/Reanalysis I [*Kistler et al.*, 2001], respectively, were probably adequate for soil moisture calculations for the US and global land,

respectively. The lack of sensitivity to temperature relates to a negative feedback. For instance, if temperature were too high (low), evaporation would be too high (low), and soil moisture would be decreasing (increasing) erroneously. However, this feeds back negatively onto evaporation at the next time level, thereby limiting the damage done by errors in the temperature input.

[3] A recent attempt (not yet published) to include snow accumulation, snow melt, and a separate equation for frozen water substance has dramatically changed the temperature accuracy requirements for the extended H96 model. Snow accumulation and snow melt in particular are very sensitive to temperature (for obvious reasons) and any errors in temperature, especially bias, will compromise the results. Moreover, there are no feedbacks that could limit the damage. While some errors are unavoidable, the US Climate Divisions and CDAS/Reanalysis I, for different reasons, are no longer good enough. The Climate Division data fail because they have not been adjusted for elevation and tend to be too warm in high terrain, thus leading to a lack of snow pack. To correct this error would require going back to

¹Climate Prediction Center, NOAA/National Weather Service, National Centers for Environmental Prediction, Camp Springs, Maryland, USA.

²Also at RS Information System, Inc., McLean, Virginia, USA.

the station data. CDAS/Reanalysis I fails because surface data, 2 m temperature in particular, is not assimilated, so the anomalies are more typical for the free atmosphere than the near surface climate. This creates large random errors. CDAS/Reanalysis I also has a model surface elevation that differs from reality but this may be the lesser of the problems.

[4] In our work on combined global soil moisture and snow calculations, we thus needed but were unable to find a suitable gridded MMSAT data set. By suitable we mean regular and timely updates, easy access, sufficient number of available stations in real time, and at least minimal quality. The Climate Prediction Center (CPC) has a long-standing experience with its own climate “anomaly” monitoring system (CAMS) global temperature data set [Ropelewski *et al.*, 1984] but we needed total (or full) values of the temperature field, not anomalies.

[5] The specific purpose of our work is thus to generate a “suitable” MMSAT data set over land, which has both the same spatial resolution (0.5 degree) and the same temporal coverage (1948–present) as the global monthly mean land surface precipitation [Chen *et al.*, 2002] used to drive the CPC leaky bucket soil model [Fan and van den Dool, 2004]. As we shall describe in detail, we combine two existing temperature data sets, the so-called CAMS and GHCN (global historical climate network) data sets using analysis techniques with several novelties.

[6] The readers are advised that the resulting temperature data set to be described in this paper was not constructed first and foremost for climate change studies. While the GHCN component of the data has gone through most quality checks one would like to see, the CAMS component of the data (much more numerous than GHCN over the last few years) is less strictly quality controlled, although quite good.

[7] The purpose of any “analysis” is to provide meaningful estimates of a variable at locations where it is not measured. Not every follow-up investigation strictly requires an analysis onto a grid. However, to have data on a grid is certainly a major convenience. As a working definition: An analysis is a representation of spatially irregular observations onto a regular grid. Moreover, a good analysis system is capable of dealing with data coverage that varies over time.

[8] The analysis of temperature is at the same time very easy and very difficult. The space-time continuity of temperature should help greatly in an analysis because analysis is essentially interpolation in between places where observations are taken. No such advantages exist for, say, precipitation, which is intermittent and difficult to interpolate. Temperature analysis is also easy because of considerable correlation in space, *i.e.*, anomalies (departures from the mean) are large-scale, both in the horizontal and to a certain degree in the vertical. The latter consideration is important to understand why CPC’s CAMS approach works quite well, even in mountainous areas.

[9] Analysis of the terrain following variable surface air temperature, at the standard height of 2 m, is thus very easy over much of the planet. However, these advantages count for little in orographically complex terrain. Here the gradients are very large because of height variations and the observations are scarce because of uninhabitability; understandably, observations are biased toward low altitudes and

thus high temperatures. The latter introduces an obvious problem when snow is part of the calculation.

[10] The analysis of scarce data in mountainous areas requires elevation adjustments which can be tricky. In the absence of observations the lapse rate can only be a climatological guess, largely ignoring daily and annual cycles, inversions in valleys, etc. Moreover, accounting for the difference between the elevation of a station (or interpolated elevations of several/many stations) and the elevation assigned to a grid point is somewhat ambiguous because the Earth’s orography at low-resolution grids may be smooth compared to reality. Beyond resolution itself it even matters where the grid points are, *i.e.*, where the origin of the grid is situated. Indeed it is difficult to get every mountaintop (or every snowfield at high elevation) close to a grid point, unless we strive for infinite resolution.

[11] Because of the orographic difficulties the original CAMS method analyzes only anomalies, leaving aside how one deals with the more constant components of the temperature field (the climatology). The assumption in CAMS is that no orographic adjustment is needed at all for the anomalies. Here we describe how we retooled CAMS into a system yielding total values, addressing orographic adjustment in the climatology. The analysis process uses both an adjusted and unadjusted climatology.

[12] Section 2 explains the data input, some ~10,978 stations, as well as the analysis method in detail, and quality checks. Section 3 describes topographic adjustment used in this study and section 4 gives a few preliminary comparisons to other data sets and Reanalyses, and concluding remarks are in section 5.

2. Data Source and Analysis

[13] The input station data sets are discussed first, and then the analysis technique to arrive at a gridded representation of the data follows in detail.

2.1. Station Data Sets and Data Quality Control

[14] Two MMSAT station data sets are used. The first is the Global Historical Climatology Network version 2 (GHCN-v2.mean, hereafter referred to as GHCN) MMSAT dataset, which was released in 1997 [Peterson and Vose, 1997; Easterling *et al.*, 1996]. The GHCN has more than 30 diverse data sources, up to 7280 stations globally and a century-plus timescale (starting from 1880, but different stations might only have data during a certain period so that the total number of available station data at any given time is less than the total station number (7280) and this becomes more clear after 1991). The GHCN has homogeneity adjustments and better quality control than its previous version 1. It will not only be regularly updated but also have additional stations added to the data set, when appropriate. The second MMSAT station data set is the Climate Anomaly Monitoring System (CAMS) data set [Ropelewski *et al.*, 1984] in use at the Climate Prediction Center (CPC) of the National Centers for Environmental Prediction (NCEP). The CAMS was designed to monitor the initiation and evolution of significant land surface parameter anomalies with high-quality, near real time observations backed by sufficiently long historical records. The CAMS data set has up to 6158 stations globally with some stations starting in the 19th

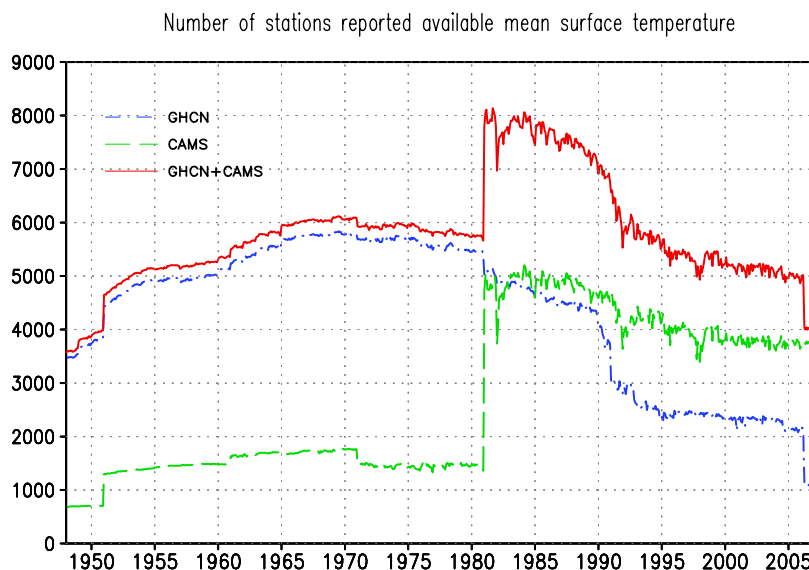


Figure 1. Number of the station reports on monthly mean surface air temperature from the Global Historical Climatology Network version 2 (GHCN) (blue dot-dashed) and the Climate Anomaly Monitoring System (CAMS) (green dashed) networks and their combined results GHCN + CAMS (red solid) with duplicate stations removed.

century. The CAMS station observations are based on two data sources; one is from the historical records collected and edited by the National Center for Atmospheric Research (NCAR) for the period before 1981. The other data, obtained on a real-time basis, is from the Global Telecommunication System (GTS) for the period after 1981. The CAMS data set also is regularly updated, in real time that is. The CAMS data is, in general, not quality controlled at the same level of sophistication as the GHCN.

[15] Figure 1 presents the time series of the number of available stations reporting MMSAT from the GHCN, the CAMS networks, and their combined results (GHCN + CAMS) for the period of 1948 to last month, where duplicate stations have been removed. It shows the GHCN data set has much more available stations than the CAMS data set before 1981 and most of the early CAMS data duplicates the GHCN. Then both the GHCN set and the CAMS data sets contain a similar amount (around 5000) of station data between 1981 and 1990 and more than half of the data are not duplicates. After 1991, the CAMS network collects considerably more station data than the GHCN. This is very important for real time updates.

[16] Some quality controls are done routinely by the CPC for the CAMS data, such as when monthly data is calculated from daily GTS data and if the station has missing data for a certain number of days (e.g., 3 d for surface air temperature and 1 d for precipitation) in a month, this station will be excluded from the data set in this month. Also to maintain homogeneity and remove outliers, some station data quality controls are further performed here for the CAMS data set, including (1) a test on unreasonable values, such as if $T \geq 60^{\circ}\text{C}$ or $T \leq -89^{\circ}\text{C}$, then reset as undefined values, (2) anomaly values which are (1) four standard deviation or more away from the mean (seasonally dependent) and (2) in absolute value larger than T_c (here T_c is latitude-dependent positive number with a small value in low latitude and a

large value in high latitude) are reset as undefined values. A bias check for discontinuity of time series will be considered in the near future.

2.2. Merging GHCN and CAMS Data Sets

[17] Figure 2 illustrates the spatial and temporal distribution of the GHCN and the CAMS MMSAT data sets. Overall, the GHCN MMSAT data set has a better data density (coverage) than the CAMS data set before 1981 and the best station networks of the GHCN stations are located in the US, while the CAMS MMSAT station networks collect more data than the GHCN after 1990 and most of the CAMS stations reside in Europe, Russia and China. The CAMS MMSAT station network also picks up more data in Africa and South America than the GHCN station networks after 1992.

[18] Since the GHCN and CAMS data sets collect data from different sources, the data coverage (i.e., station locations and period of data collected) from the two data sets may be different, even for the duplicate stations. In general, the GHCN data set collects more data than the CAMS before 1981 and quickly drops after 1991. The CAMS data set collects more data than the GHCN after 1981 (by the time CPC started to archive GTS data) and it stays relatively stable in the real time update.

[19] To take advantage of both data sets, the following method was used to merge the two data sets and eliminate as much duplication as possible. The merging methodology is a three-step process: First, the data before 1948 in the GHCN has been ignored here, and second, the two data sets have been reorganized so that both the data sets have a similar data structure and starting and ending time points and are thus easy to merge. Third, for those stations in the two data sets which have the same World Meteorological Organization (WMO) station identification number, a match checking for both the station distance and temporal correlation has been conducted. Whenever the two stations with

Location and Density of Mean Temperature Stations

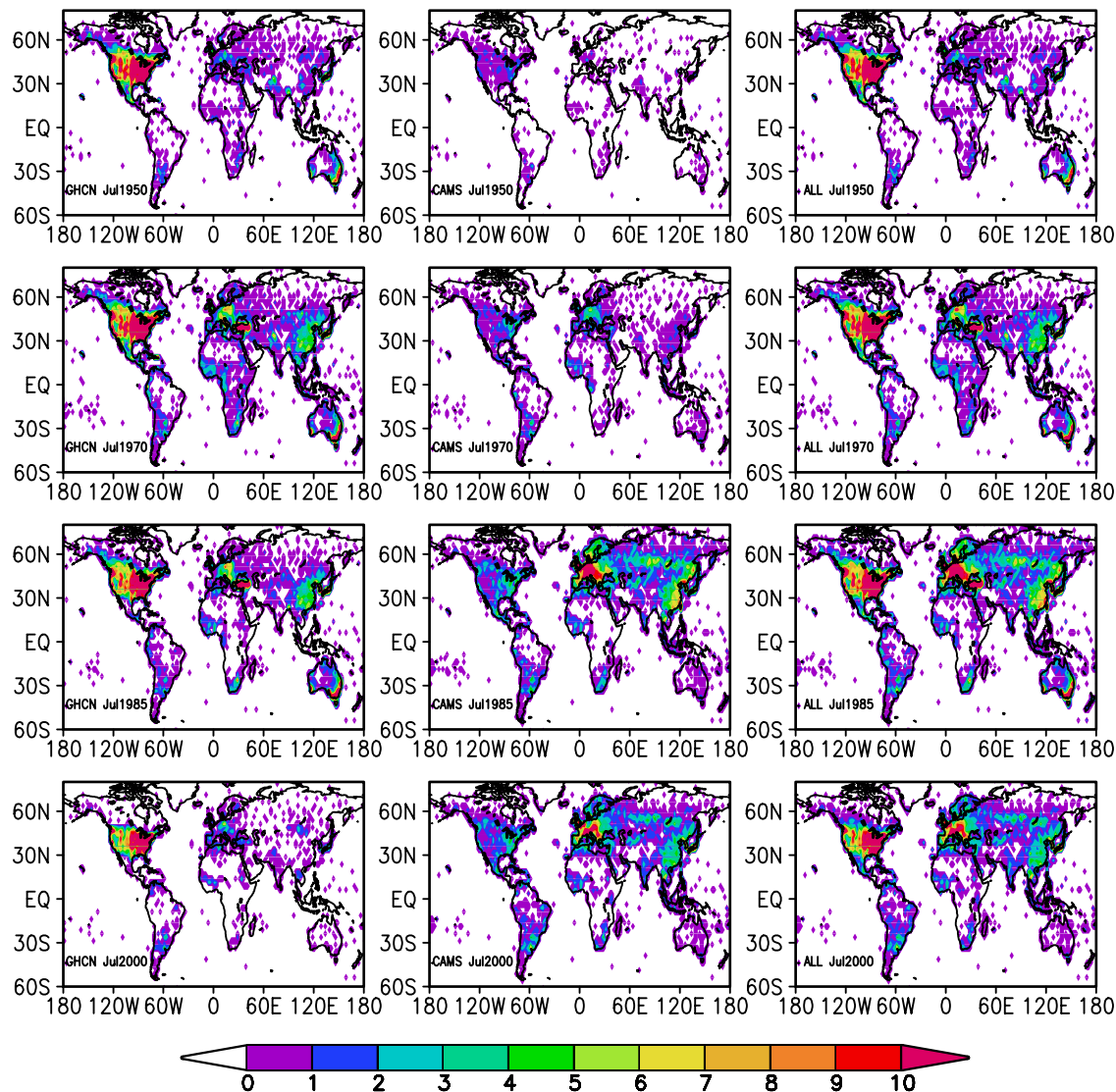


Figure 2. Location and density (number of stations in one grid box) of the monthly mean surface temperature stations in July of selected years, (top to bottom) 1950, 1970, 1985, and 2000, from (left) GHCN, (middle) CAMS, and (right) their combination.

the same WMO identification number fall in the following situations: (1) differences of latitude and longitude are both less than 0.1 degree and (2) the temporal correlation of the two station data sets is larger than 0.9, then a match (or duplication) is declared. Under these criteria, there were 2460 duplicate stations and 3698 nonduplicate stations in the CAMS data sets. Therefore the total number of non-duplicate stations from the GHCN and CAMS merged data sets is 10,978.

[20] For the duplicate stations, if both stations have no missing data, the station data of the GHCN will be kept and the CAMS station data will be set to undefined data. If some of the GHCN station data is missing and the CAMS station data is available, the CAMS station data will be used to replace the GHCN station data. In this latter scenario (i.e., GHCN missing and CAMS existing for the duplicate stations), there were 1133 stations which were patched with

more than 100 months of the CAMS data and 185 stations that were patched with more than 200 months of the CAMS data for the period of 1948 to present month. Since many stations only have reports during a certain period, the total number of available station reports in each month is always smaller than the total available 10,978 stations and, in fact, never exceeds 8100 (see Figure 1).

[21] The above results show that the CAMS data set not only brings in about 3700 new stations which the GHCN data set does not have at all but also patches many missing data points for duplicate stations in the GHCN data set. The stable data collection underlying the CAMS data set after 1981 plays a crucial role for near real time updates.

2.3. Algorithm for Analysis

[22] Several algorithms, from the Thiessen's polygon [Hulme, 1992], the thin-plate spline-fitting [New *et al.*,

1999], the optimal interpolation [Gandin, 1965; Reynolds and Smith, 1994; Chen et al., 2002], to the least squares distance weighting, etc. [Cressman, 1959; Ropelewski et al., 1985; Higgins et al., 2004] have been used to interpolate irregularly distributed meteorological station data to a grid. An overview of common data interpolation techniques and some major spatial climate-forcing factors can be seen in Daly's [2006] paper. Here the Cressman based objective analysis scheme, which is built into the Grid Analysis and Display System (GrADS), is used on the merged GHCN + CAMS station data to generate 0.5 latitude by 0.5 longitude gridded results. The scheme uses multiple passes through the grid at subsequently lower radii of influence. The first guess value of the analysis grid is set to the arithmetic average of the observations in the area. For each pass, a new value is determined for each grid point by arriving at a correction factor for that grid point. This correction factor is determined by looking at each station within the radius of influence from the grid point. For each such station, a discrepancy is defined as the difference of the station value and a value interpolated from the nearby grid to that station. Then a distance weighted formula is applied to all such discrepancies within the radius of influence of the grid point to arrive at a correction value for that grid point. A number of combination radii of influence are tested and one group with nine passes which gives the best gridded data coverage (i.e., no holes at all or it keeps the number of holes to a minimum and at the same time preserves the fine spatial structure) is chosen and then used for the entire analysis.

[23] Normally, two approaches can be used to interpolate irregular station observations to a regular spatial grid (here global 0.5×0.5 degree high resolution). The first and conceptually the easiest approach is to interpolate "full" station temperature (total values) directly to the grid. However, this approach has some limitations and is only good for areas having a spatially and temporally dense station network with small gradients. For areas having only a few stations or in mountainous areas with a lot of missing data in time, the full (value) approach may generate large errors in the interpolated temperature fields. An alternative to the full approach is the anomaly approach (as seen in the name CAMS). This approach is based on the assumption that the monthly temperature anomalies tend to be large scale and relatively independent of topographic control. Therefore the anomaly interpolation should yield more accurate results than the full value interpolation approach. A further discussion about the two approaches can be found in section 2.4. The amended anomaly approach, with some unique features and the purpose of obtaining full values at the end, is followed here and involves five steps that can be described as follows:

[24] 1. A gridded 30-year mean monthly climatology is constructed by using the Cressman objective analysis scheme described in the above, based on the merged GHCN + CAMS MMSAT station data for the period from 1961 to 1990, which has relatively better station data coverage over the globe during this period. Then the station mean monthly climatology is obtained by bilinearly interpolating the above gridded mean monthly climatology back to the given station locations within the grid space. One advantage of doing it this way is that every station data passed quality control is used and stations with missing data during some months or

even the whole period of 1961–1990 may still get a 1961–1990 station climatology (i.e., obtain data by interpolation from nearby stations). Since no terrain adjustment was done as yet to the above gridded climatology and station climatology, both of them are referred to as the unadjusted climatologies.

[25] 2. The anomalies of the station MMSAT data are determined by subtracting the above unadjusted station MMSAT climatology. Next, the station monthly anomalies are interpolated to the grid. To produce the full MMSAT, the gridded anomaly fields obtained here, together with the unadjusted MMSAT gridded climatology fields from step 1, are combined to deliver the full values of (no elevation adjustment) gridded temperature analysis. The values of the gridded temperature analysis are representative for the grid points (i.e., not meant as grid box average).

[26] In order to refine both the above unadjusted gridded and station climatologies, procedure 2 above can be repeated many times, where in the first round the unadjusted climatologies will be calculated from step 1, i.e., the full value interpolation. In the next few rounds the unadjusted climatologies will be obtained from procedure 2, i.e., the anomaly interpolation approach assuming anomaly interpolation will generate more accurate results. Eventually the interpolated value on each grid or station will converge to a certain number.

[27] 3. Here, a terrain adjustment is applied to the above gridded mean monthly unadjusted climatology to derive the adjusted climatology. The difference between the interpolated (reported) station elevation and the grid elevation is multiplied by the spatial-temporal varying near surface air temperature lapse rate and added to the unadjusted climatology, see section 3 for more detail.

[28] 4. Another MMSAT climatology on exactly the same 0.5×0.5 grid as the above GHCN + CAMS grid, based on more than 12,000 station mean monthly temperature normals collected by the Climate Research Unit (CRU) of University of East Anglia, United Kingdom for period of 1961–1990 [New et al., 1999], is used to repair the holes in the gridded GHCN + CAMS MMSAT climatology in areas where there is not enough station data available to us, such as a tiny hole in the Sahel and a large portion of north and central Greenland.

[29] 5. To produce the elevation-adjusted full MMSAT, the gridded anomaly fields obtained in step 2, together with the elevation adjusted MMSAT climatology fields from steps 3 and 4, are combined to deliver the final full values of gridded temperature analysis.

2.4. Analysis Quality Checks

[30] A few methods are used here to check the quality of the analysis. First, as a sanity check for the Cressman analysis used in this study, the gridded MMSATs with the full value interpolation and anomaly interpolation (no terrain adjustment applied) are returned to the station locations at different time points (see Figure 3 as an example). The differences between the returned values from gridded data and the original station values are almost zero in most areas (see Table 1 for statistical results based on the 30 year (1961–1990) period), except in the areas with poor spatial and temporal data coverage and land/water boundary, as it should.

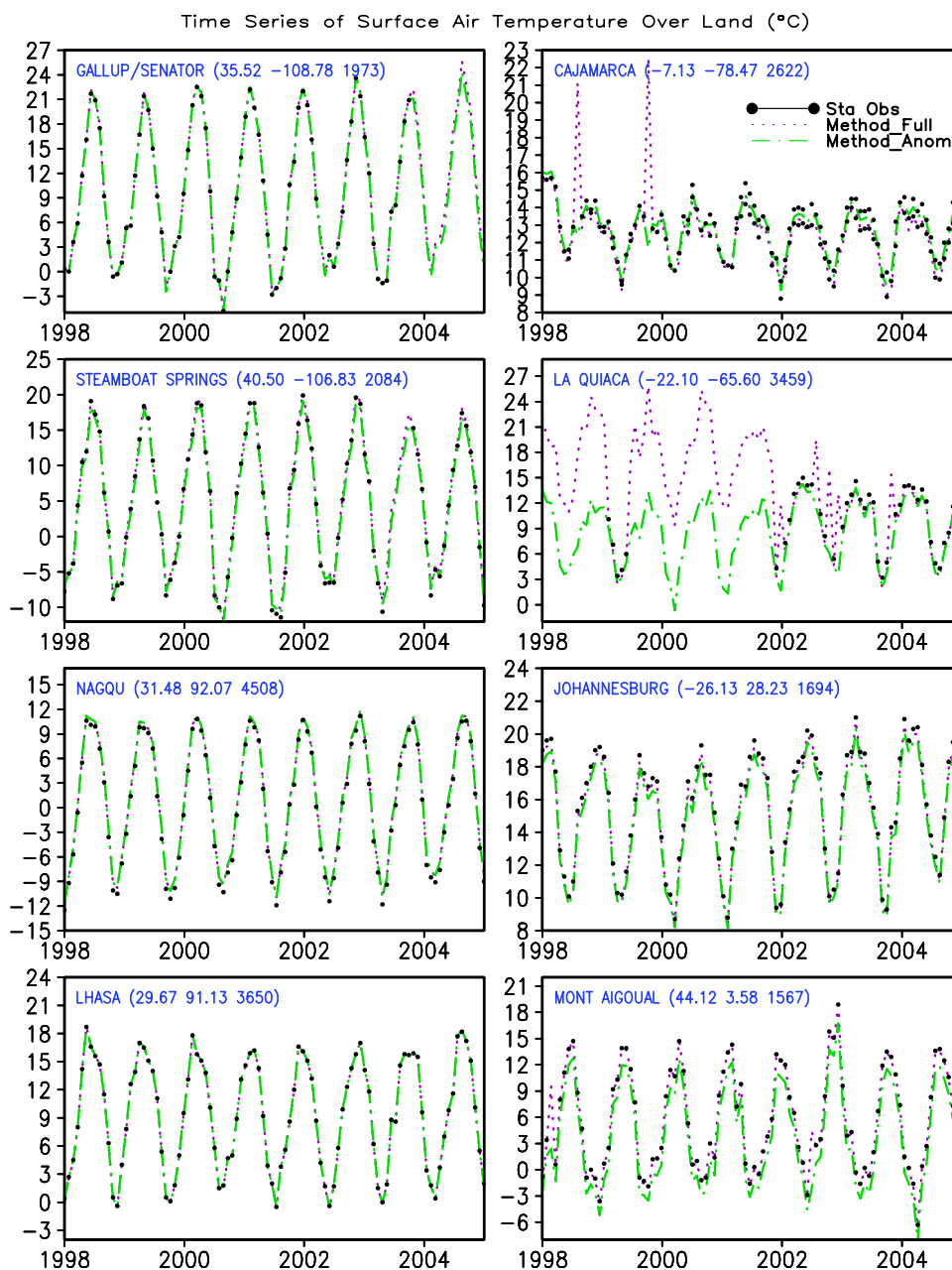


Figure 3. Time series of the surface air temperature at some randomly selected high-elevation stations. Closed circle represents observed station value, dotted line represents full value interpolation, and dot-dashed line represents anomaly interpolation.

[31] An intercomparison between the full value interpolation and anomaly interpolation (yielding full values at the end) has been conducted over the global domain. In general, the interpolation of anomalies generates fewer “bull’s eyes” and yields better patterns and amplitude of anomalies. The statistical analysis (see Table 1 and Table 2) also shows

similar results. Figure 3 displays the time series of the surface air temperature at some randomly selected high-elevation stations for both full value interpolation and anomaly interpolation (no topography adjustment was done for either interpolation approach yet). The comparison indicates that over the area having better station network

Table 1. Data Validation Over Global Land for the Period of 1961–1990^a

Interpolation Method	Correlation	rmse	Bias
Full interpolation	0.97	0.18°C	-0.001°C
Anomaly interpolation	1.00	0.16°C	-0.004°C

^aHere quality is measured by anomaly correlation (station versus interpolated grid), root mean square error (rmse), and bias.

Table 2. Cross-Validation for Reduced Station Network Density Over Global Land for the Period of 1961–1990^a

Interpolation Method	Correlation	rmse	Bias
Full interpolation	0.76	1.18°C	-0.016°C
Anomaly interpolation	0.80	1.03°C	-0.008°C

^aHere quality is measured by anomaly correlation (station versus interpolated grid), root mean square error (rmse), and bias.

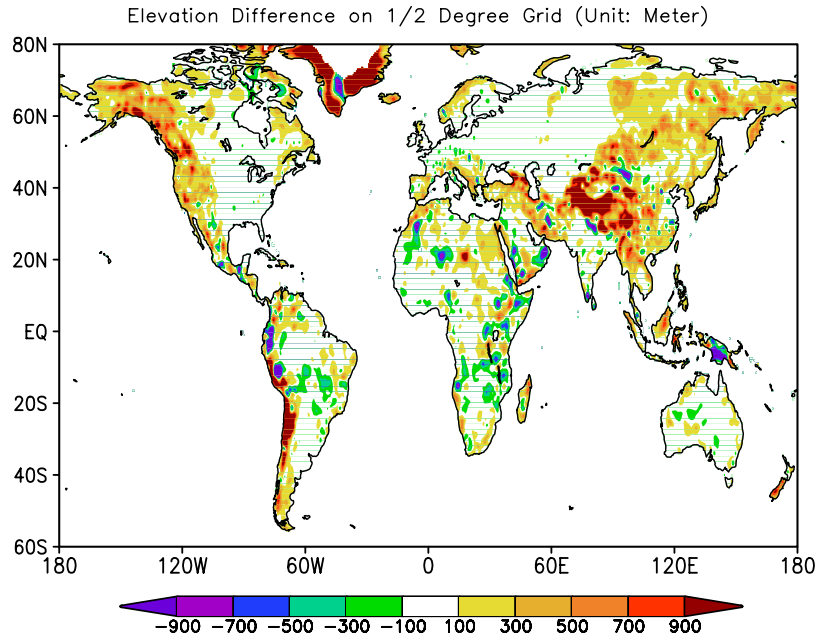


Figure 4. Elevation difference (in meters, and negative values are inside the dashed contour) between the 0.5×0.5 topography used here and the gridded GHCN + CAMS station elevation.

and less missing data the results from the two interpolation methods are very similar. However, over the region with sparse station network coverage and more missing data in time, the results show that the anomaly interpolation yields better phase evolution and more accurate amplitudes of the surface air temperature, while the full value interpolation produces, on occasion such as in cajamarca, large errors.

[32] Also to examine the impact of varying station network density on the accuracy and sensitivity of the interpolated MMSAT, one simple intercomparison has been made by removing about 200 available stations over the global land area from the analysis by raising the matching (or duplication) criteria. The difference of the two gridded MMSAT datasets are quite small and no serious degradation is found due to decreasing the number of available stations. Another cross-validation was conducted by randomly separating the total number of stations (10,978 here) into ten groups and then withdrawing the data from one group (10%) one at a time and comparing it with the analysis from the remaining 90% of station data at locations of the withdrawn stations. This process was conducted 10 times so that it guarantees each station was withdrawn once. Table 2 shows that the interpolation accuracy degrades the reducing the station network density. In general, accuracy decreases more seriously in areas with poor spatial and temporal data coverage and near land/water boundary (not shown). The accuracy of the GHCN + CAMS analyses should be close to the results in Table 2. However, keep in mind that the uncertainty of 1°C comes about from very large areas with a few tenths uncertainty and small areas with huge errors.

3. Topographic Adjustment

[33] Among many common spatial climate-forcing factors, terrain or orography features can heavily affect the spatial patterns of some meteorological variables, such as precipitation, surface air temperature, radiation, humidity,

etc. Sometimes steep gradients or large spatial variations can be found over short distances. In regions with significant and complex terrain, surface air temperature usually exhibits predictable (decrease or increase) variations with elevation. Therefore interpolation of these meteorological variables accounting for the impact of topography is necessary, if the station elevation is different from the interpolated grid elevation.

[34] In this paper, a topography adjustment, which depends on the elevation differences and the nearby surface air temperature lapse-rate, is used based on

$$T_{grid} = T_{sta} - \gamma \Delta Z \quad (1)$$

where T_{grid} is the adjusted gridded surface air temperature and T_{sta} is the surface air temperature on the same grid as T_{grid} but gridded from the merged GHCN + CAMS station data, γ is the temperature lapse rate and $\Delta Z = Z_{grid} - Z_{sta}$, where Z_{grid} is the 0.5×0.5 topography (interpolated from a global digital topography at 0.083333×0.083333 degree resolution, which originates from the U.S. Geological Survey Digital Elevation Model data and is considered as true elevation), and Z_{sta} is the GHCN + CAMS reported station elevation analyzed onto the same 0.5×0.5 resolution and represents the topography of the station networks. Some common spatial climate forcing factors, such as coastal effects, land surface character (i.e., bare soil, vegetation, and forest), and the orientation, position, and barrier of terrain, are ignored. Figure 4 shows the land surface elevation difference ΔZ , defined as in equation (1). Significant elevation differences can be seen in the major mountainous areas. Therefore topographic adjustment in those areas is necessary.

[35] Typically, the dry adiabatic lapse rate γ_d is 9.8 deg/km . The moist adiabatic lapse rate γ_m depends on the amount of moisture present and varies from 3 to 7 deg/km in the lower troposphere. It is known that the actual temperature

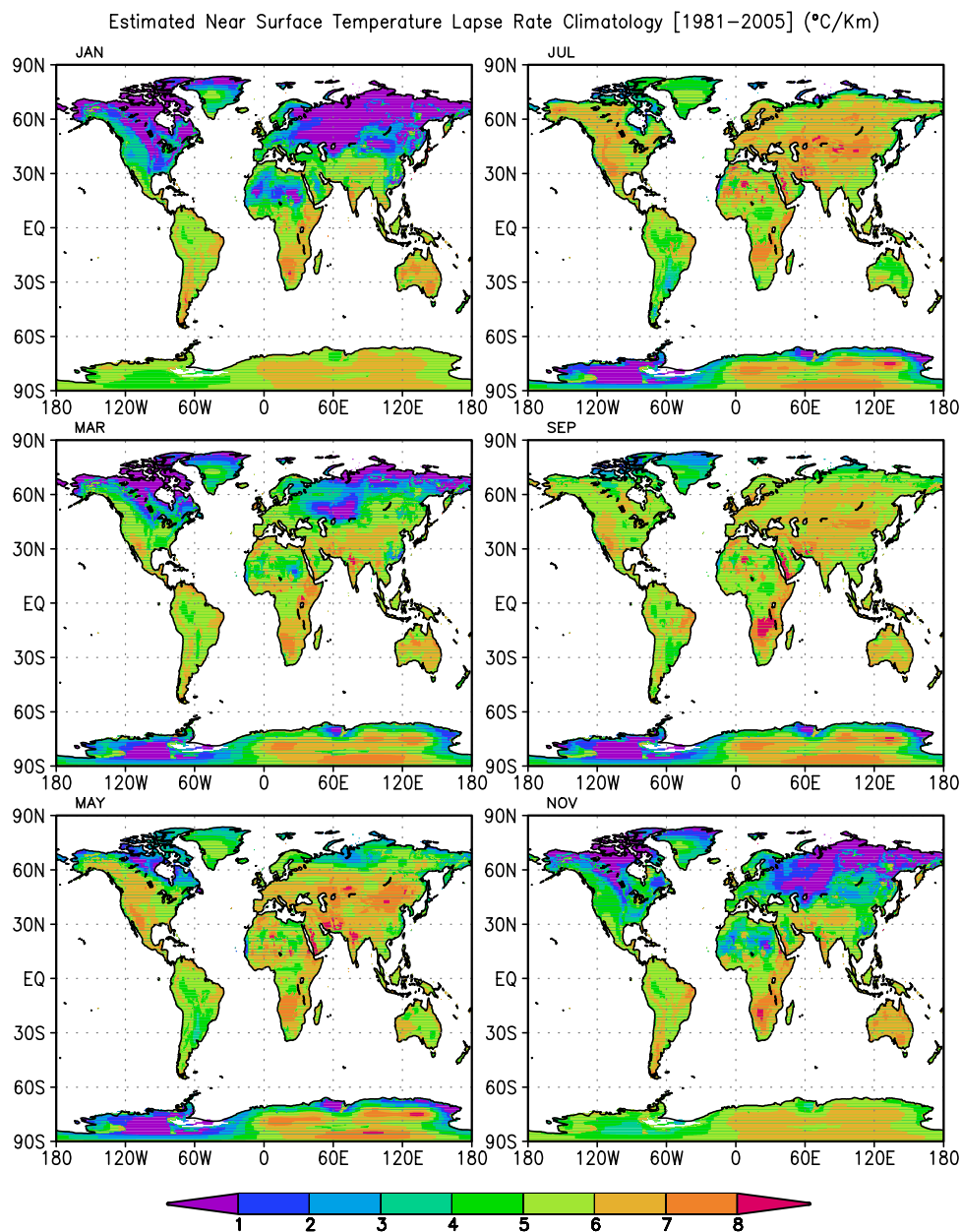


Figure 5. Global monthly mean near surface air temperature lapse rate climatology (in $^{\circ}\text{C}/\text{Km}$), for 6 selected months, estimated from the National Centers for Environmental Protection–Department of Energy global Reanalysis for period of 1981–2005.

lapse rate not only has a diurnal cycle but also varies with space and season [Bolstad *et al.*, 1998; Rolland, 2002]. Figure 5 presents a monthly global near surface air temperature lapse-rate climatology, estimated from NCEP-DOE global Reanalysis temperature fields and geopotential height fields at 1000 hPa, 925 hPa, 850 hPa, 700 hPa, and 600 hPa for the period of 1981–2005. Together with the topography Z_{grid} , the surface air temperature lapse-rate γ was selected from the nearest layer. Some typical features can be seen, such as in general, surface air temperature lapse rates over land have much larger seasonal variation than those over the ocean (not shown over the ocean). Over land the surface air temperature lapse rates in the warm season and low latitude are larger than those in the cold season and high latitude.

The seasonal evolution of the monthly surface air temperature lapse-rate climatology obtained here are comparable with those calculated from scarce observations [Harlow *et al.*, 2004].

[36] Figure 6 shows the seasonal cycle of the merged GHCN+CAMS surface air temperature climatology with and without topographic adjustment, together with the widely used CRU [New *et al.*, 1999] surface air temperature climatology and the Parameter-Elevation Regressions on Independent Slopes Model (PRISM group, Oregon State University, see <http://www.prismclimate.org>) surface air temperature climatology over the western U.S. mountain region for the period of 1961–1990. It shows the evolution of merged GHCN + CAMS surface climatology (with

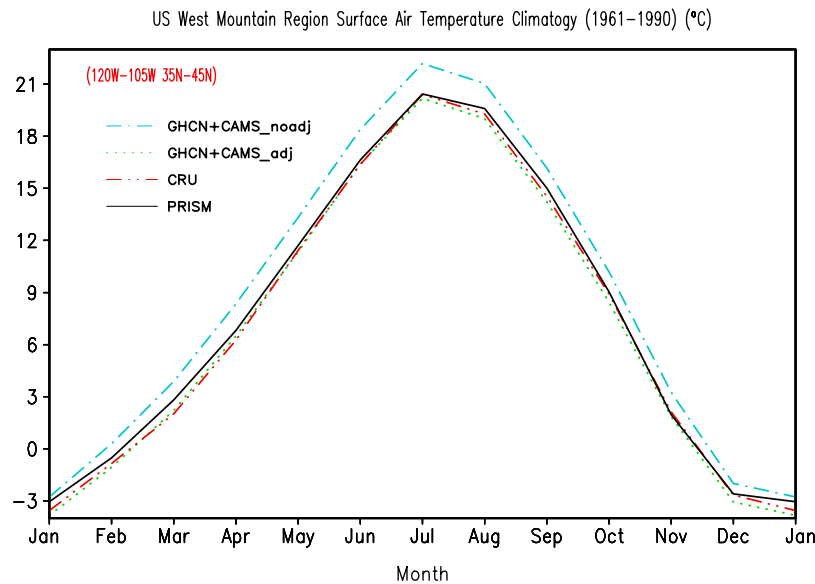


Figure 6. Seasonal cycle of the gridded GHCN + CAMS surface air temperature climatology, Climate Research Unit (CRU) surface air temperature climatology, and Parameter-Elevation Regressions on Independent Slopes Model (PRISM) surface air temperature climatology averaged over the U.S. west mountain area ($120^{\circ}\text{W}–105^{\circ}\text{W}$, $35^{\circ}\text{N}–45^{\circ}\text{N}$) for the period of 1961–1990. Solid line is the PRISM data, dotted line is the merged GHCN + CAMS data with topography adjustment, dot-dashed line is the merged GHCN + CAMS without topography adjustment, and dot-dot-dashed line is the CRU data.

topographic adjustment) agrees with the PRISM climatology and the CRU climatology quite well. The small differences among the three data sets suggest that there is uncertainty due to the methods used to generate the data sets, different data sources and the topography represented by their respective grids. Clear differences are found between the merged GHCN + CAMS surface air temperature climatologies with and without topographic adjustment. The unadjusted GHCN + CAMS data set is warmer than the adjusted GHCN + CAMS data sets, which indicates many stations in the western U.S. mountainous regions are either in the valley or at lower elevation. In general, the difference of the unadjusted and adjusted GHCN + CAMS datasets are smaller in the cold season (low lapse rate) than the warm season (high lapse rate), indicating the topographic adjustment is more important for the warm season.

[37] As a cautionary comment for the above terrain difference between the two elevation data sets, an artificial error (or adjustment) may be induced on the grid when the station is exactly on the grid (in terms of latitude/longitude) but with a different surface elevation. If not specifically mentioned otherwise, all following gridded GHCN + CAMS results are derived from the anomaly interpolation approach and topographic adjustment scheme defined here with the above topography difference and space-time varying surface air temperature lapse rate.

4. Preliminary Results

4.1. Comparison With PRISM MMSAT

[38] At lower elevation in areas covered by a dense station network, different surface air temperature data sets, such as the merged GHCN + CAMS, PRISM, and CRU

data sets, are very close to one another. The real challenge is in the mountainous regions with sparse station network. Figure 7 shows the January and July spatial distribution of the surface air temperature climatology from the merged GHCN + CAMS data sets, and from the PRISM surface air temperature data set, and their differences for the respective months. (The PRISM data has been regridded to the GHCN + CAMS grid for the purpose of producing the difference maps.) The PRISM data set used here is derived from a more complicated interpolation technique and has much higher (4 km) resolution. The results show that the major patterns of the GHCN + CAMS and PRISM data sets are similar and the elevation adjusted GHCN + CAMS data set is more in agreement with the PRISM data set than the unadjusted GHCN + CAMS (not shown). However, clear differences (around 2° to 4°C) between the GHCN + CAMS and PRISM data sets are found in the western U.S. mountainous regions, and the structures of the differences switch between the January and July patterns. In general, the differences in the eastern US are smaller (less than 0.5°C) for all months (not shown). These differences are due to different data sources, interpolation methods, data resolutions, and the adjustment itself.

4.2. Comparison to the National Climate Data Center (NCDC) Climate Division Data

[39] In this section, the NCDC 344 climate division MMSAT data set over the conterminous U.S. was compared to the gridded GHCN+CAMS MMSAT. Figure 8 illustrates the 30 year climatology for January and July averaged for the period of 1961–1990, and their difference for the respective months (here the NCDC climate division data has been interpolated to a 1×1 degree grid and the GHCN +

Jan & Jul GHCN+CAMS and PRISM Temp Climatology [1961–1990] and Their Differences (°C)

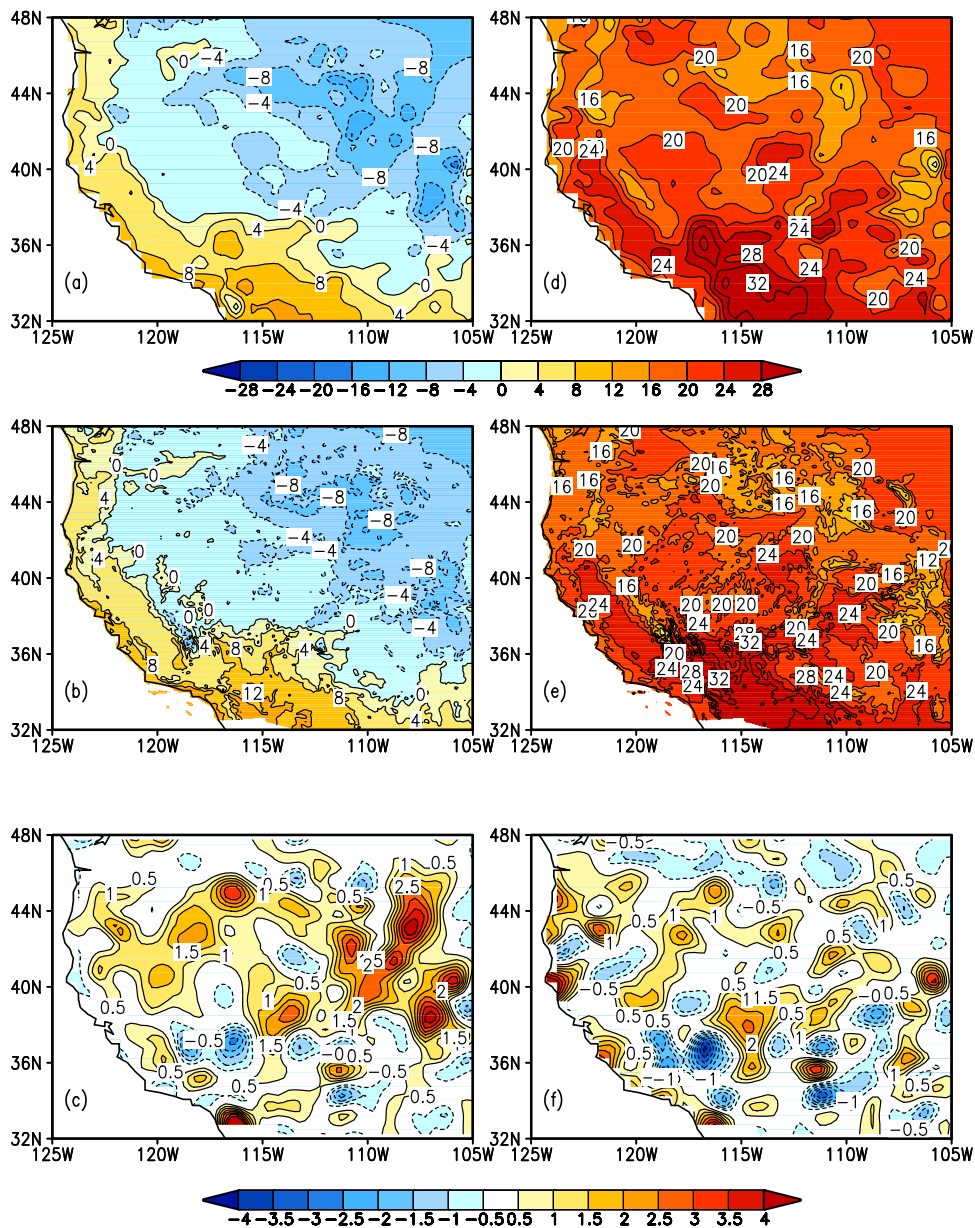


Figure 7. Gridded (top) GHCN + CMAS and (middle) PRISM surface air temperature climatology (in °C, and negative values are inside the dashed contour) for 1961–1990 and (bottom) their differences (PRISM minus GHCN + CAMS) for (left) January and (right) July over the U.S. west mountain area.

CAMS data has been regridded to the same grid). The major patterns and even some fine structures of the climatology from the two data sets are very similar to each other. However, larger differences can be seen in the western US mountainous region, where the climate division data can be more than 4°C warmer. The main reason for the differences is that the climate division data (an average of all data within the climate division) does not have enough resolution to represent the small structures of the surface temperature in complex orographic areas, nor do the CD data have an elevation adjustment.

[40] Time series of surface air temperature anomalies and their annual cycles averaged over the western U.S. moun-

tainous region and the eastern U.S. plain over the whole period of 1948–present month reveal that the temperature anomalies and the annual cycles of the two data sets (Climate Divisions and GHCN/CAMS) follow each other very closely (not shown). Over the western U.S. mountainous regions the (pointwise) anomaly correlations of the two data sets for the period 1961–1990 range from 0.86 to 0.98, and over the eastern US plain the average is 0.99. As in the above, large differences (average about 3°C bias in summer and 1°~2°C bias in other seasons, indicating again the topography adjustment is more important for the warm season) are found in the mean surface air temperature over the U.S. west mountain region. This suggests that the

Jan & Jul GHCN+CAMS and NCDC_CD Temp Climatology [1961–1990] and Their Differences (°C)

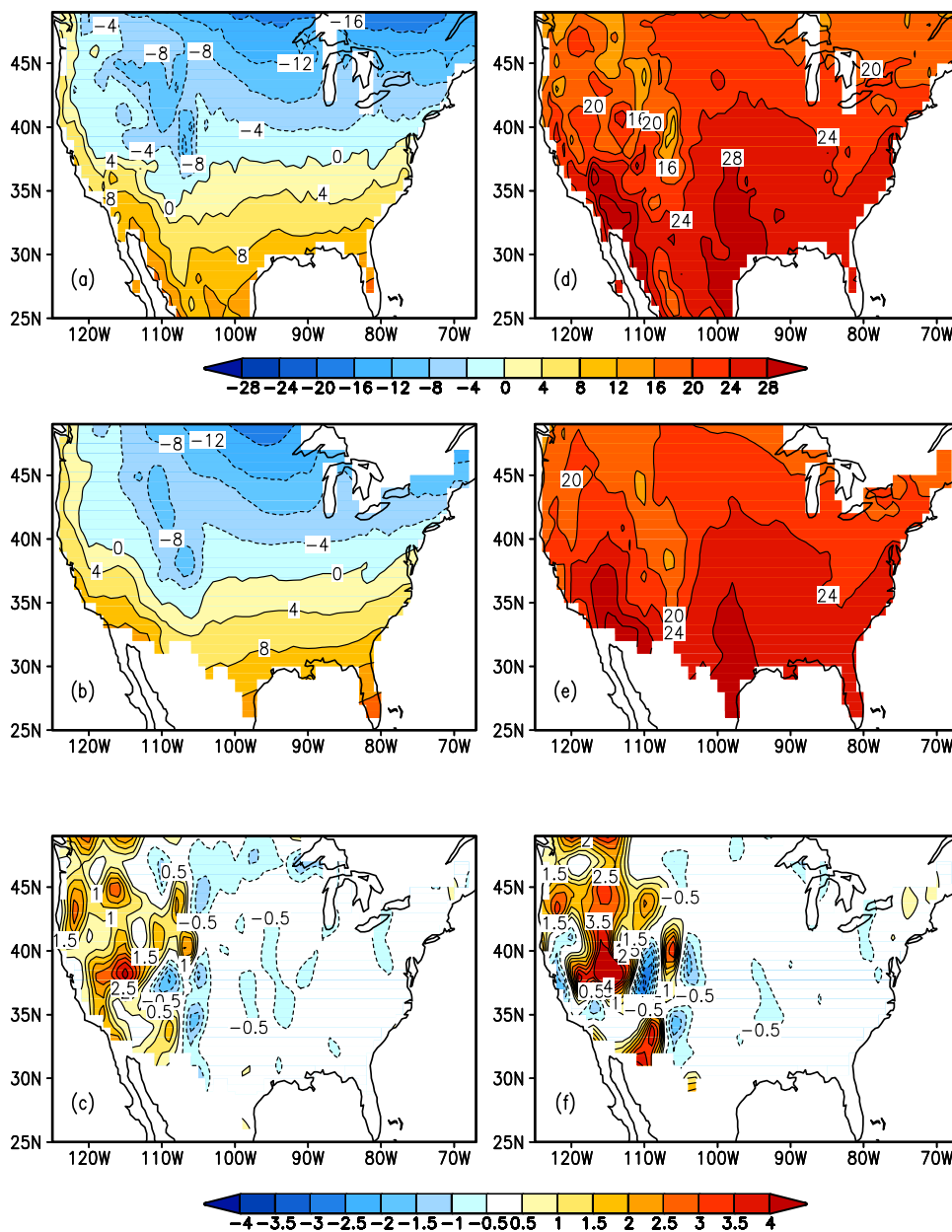


Figure 8. Same as Figure 7 but for the gridded GHCN + CMAS and the NCDC climate division surface temperature climatology (in °C, and negative values are inside the dashed contour) for 1961–1990 over the conterminous United States.

NCDC climate division MMSAT data can catch the large-scale surface air temperature anomalies very well (although not quite as good in the mountains as over simpler terrain) but fails in the absolute values.

4.3. Comparison to the CRU Climatology

[41] The CRU MMSAT climatology for the period of 1961 to 1990 is used to validate the merged GHCN + CAMS MMSAT climatology for the same period. The two data sets are already on the same grid, i.e., no regridding is required. The seasonal evolution of spatial patterns for the gridded GHCN + CAMS and CRU surface MMSAT climatology closely follow each other (not shown). For all

months, all major patterns over the globe in both higher and lower latitudes, and even most of the fine structures in the mountainous areas of the two MMSAT climatology data sets are very similar. The annual cycles of the merged GHCN + CAMS and CRU MMSAT averaged over the Northern Hemisphere and Southern Hemispheres, respectively, follow each other very closely in both phase and amplitude (see Figure 9), with CRU MMSAT slightly colder in the Northern Hemisphere and slightly warmer in the Southern Hemisphere in the boreal spring and winter. For the zonal mean, the two data sets agree with each other reasonably well, but some differences are seen and they vary with locations and seasons.

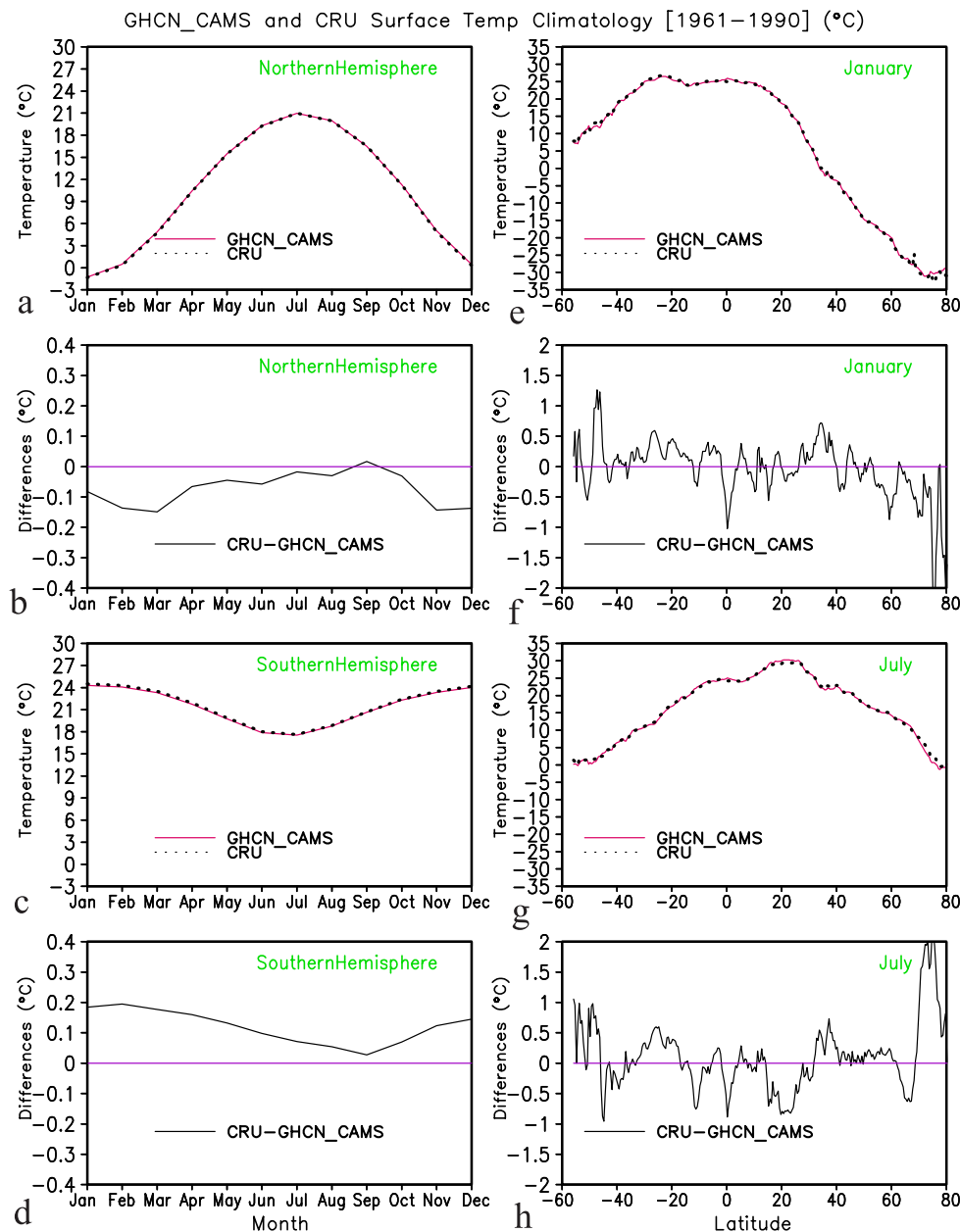


Figure 9. Annual cycle of the merged GHCN + CAMS and CRU monthly mean surface air temperature (MMSAT) climatology (1961–1990) averaged over the (a) Northern Hemisphere [0° – 360° E, 0° – 80° N] and (c) Southern Hemisphere [0° – 360° E, 0° – 60° S] and (b,d) their differences. Also shown are (e–h) zonal mean MMSAT of the above climatologies and their differences for January and July.

[42] The differences between the merged GHCN + CAMS MMSAT seasonal mean climatology and the CRU MMSAT seasonal mean climatology are depicted in Figure 10. It shows that in most areas with a better station network coverage the differences between the two climatology data sets are very small. The major differences appear in the high mountainous areas where the observations are also scarce. These differences could be resulting from using different interpolation schemes, different elevations, and/or different elevation adjustments and different data sources. The other areas having relatively large differences are located in the uninhabited desert regions and high latitudes, such as in the Andes Mountains and the Sahara region, the mountainous

area of the U.S., Canada, and into Alaska, and in the far eastern part of Russia, with a clear seasonal reversal of the sign of the difference (this may be because our orographic adjustment is more sophisticated since it has a seasonally varying lapse rate). Another possible reason for these differences is that the merged GHCN + CAMS has a slightly better station network coverage than the CRU data set over the uninhabited high-latitude regions.

4.4. Comparison to the Global CDAS/Reanalysis II and ERA40 Data Sets

[43] The CDAS/Reanalysis II [Kanamitsu *et al.*, 2002] is an updated version of CDAS/Reanalysis I [Kistler *et al.*,

Differences of CRU & GHCN+CAMS Surface Temp Climatology [1961–1990] (°C)

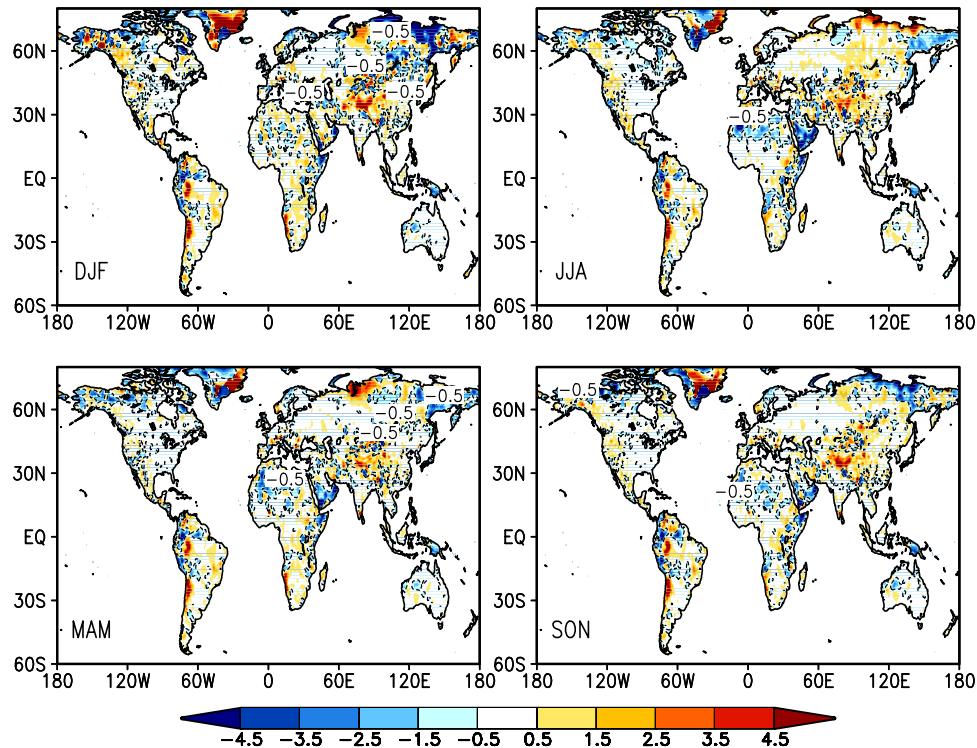


Figure 10. Difference between the seasonal mean (DJF, MAM, JJA, and SON) CRU MMSAT climatology and the merged GHCN + CAMS MMSAT climatology (in °C, and negative values are inside the dashed contour) for the period of 1961–1990.

2001] and has been widely used in diagnosis, simulation and prediction, such as in the current version of the NCEP Climate Forecast System (CFS) [Saha *et al.*, 2006], which uses CDAS/Reanalysis II for its atmosphere and land initial conditions. However, some of the CDAS/Reanalysis II variables are model generated and no observations were assimilated, such as the 2 m surface air temperature. Figure 11 depicts the difference of the CDAS/Reanalysis II MMSAT climatology and the merged GHCN + CAMS MMSAT climatology (here the GHCN + CAMS data has been regridded to the CDAS/Reanalysis II grid) over the global land portion for the common period of 1981–2005. Over the global domain, large biases can be found in both high and low elevation areas. For example, major differences (biases) are seen north of 50°N, with seasonal reversal of the sign of the bias. Over a large portion of these areas the CDAS/Reanalysis II MMSAT shows over 4°C warm biases in winter and cold biases in May and June.

[44] In the middle latitudes of the Northern Hemisphere, large (above 3°C) cold biases are found in the U.S. western mountainous areas (especially from February to May), and up to 3°C biases with seasonal reversal are seen in the eastern US, the middle and eastern Asia regions. In lower latitudes, very large cold biases (above 3°C and all year round) are located in the whole Sahara and for a large part of the Tibetan Plateau to Northern India and Bangladesh. From the tropics into the southern hemisphere, large cold biases are shown over the Amazon region in all seasons and very persistent warm and cold biases are seen along the Andes Mountains. Some moderate cold biases are also

found in the highland in the southern part of Africa during the cold season. A comparison of the NCEP-NCAR Reanalysis I against GHCN + CAMS (not shown) reveals all the same problems, but in addition some technical errors in running R1 are playing up. The snow cover/thickness of 1973 was given erroneously to many later years and this caused additional temperature problems in the NCEP-NCAR Reanalysis I.

[45] Another Reanalysis data set used here is the European Center for Medium-Range Weather Forecasts 40 year Reanalysis (ERA40) data set [Uppala *et al.*, 2005], which covers the whole time period 1958–2001. Keep in mind that as a unique feature in Reanalysis, the ERA40 T2m data was further postprocessed to ingest surface air temperature observations. Figure 12 shows the differences of the ERA40 MMSAT climatology (1981–2000) and the merged GHCN + CAMS MMSAT climatology (here the GHCN + CAMS data has been regridded to the ERA40 grid) over the global land portion for the same period of 1981–2000. Compared to the CDAS/Reanalysis II data set, the biases of the ERA40 MMSAT respective to the GHCN + CAMS data set are clearly smaller. However, noticeable and persistent biases are still found over a large portion of the high latitudes in the Northern Hemisphere, the Tibetan Plateau, the Sahara region, the equatorial Central America, and the Andes Mountains.

[46] The temporal anomaly correlations between the Reanalysis II and GHCN + CAMS data sets and between the ERA40 and GHCN + CAMS data sets over the global land surface domain for the period of January 1981 to

Difference of Reanalysis II & GHCN+CAMS Surface Temp Climatology [1981–2005] ($^{\circ}\text{C}$)

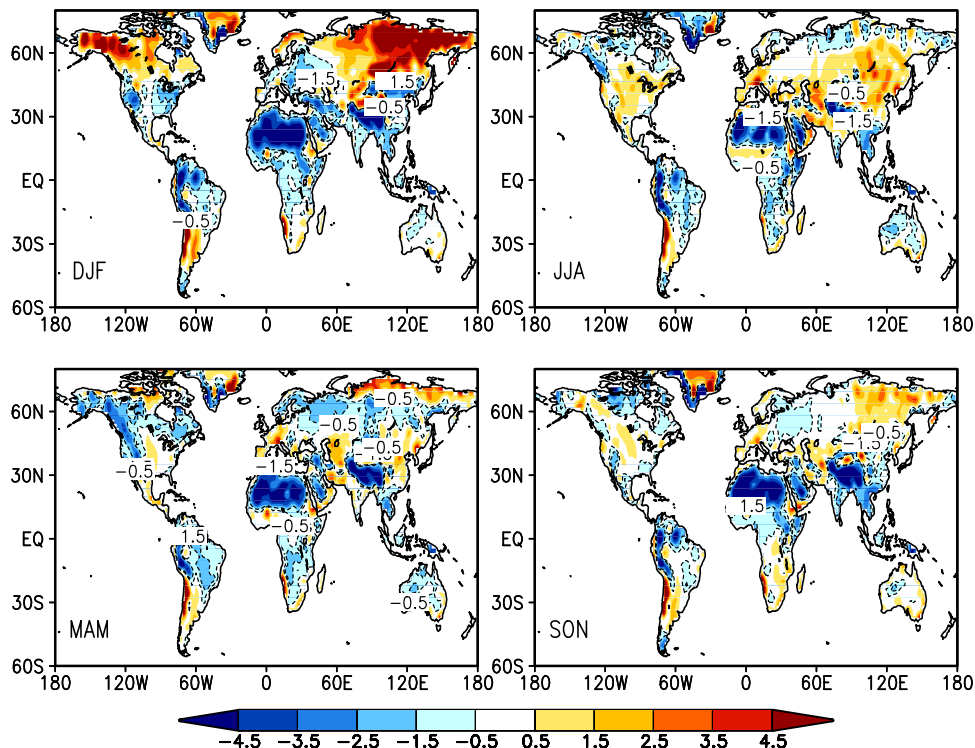


Figure 11. Difference between the seasonal mean (DJF, MAM, JJA, and SON) Climate Data Assimilation System (CDAS) II (or Reanalysis II) climatology and the merged GHCN + CAMS MMSAT climatology (in $^{\circ}\text{C}$, and negative values are inside the dashed contour) regridded to the CDAS II grid for the period of 1981–2005.

December 2000 are presented in Figure 13, which shows where the Reanalysis data sets are in good or bad agreement with GHCN + CAMS data set. In general, both Reanalysis data sets are very well correlated (>0.9) with the observations (GHCN + CAMS) over North America, Europe, Asia, and Australia, where we have good observation coverage, but note some deterioration over mountains (<0.90 or even <0.80). However, very poor correlations are found in the tropical Central America, tropical Africa, the Sahara, high mountainous regions, and a large part of Greenland. Overall, ERA40 Reanalysis did a slightly better job than NCEP-DOE Reanalysis over these problematic areas, but the basic problem is still the same.

[47] Time series of surface air temperature anomalies and their annual cycles averaged over four selected regions for the period of 1981–2000 from the above three data sets are shown in Figure 14 (for clarity, the anomalies are only shown for the period of 1991–2000). It reveals that the temperature anomalies and the annual cycles of the three data sets in the western U.S. mountainous region [120°W – 110°W , 35°N – 40°N] and the eastern U.S. plain [90°W – 80°W , 35°N – 40°N] follow one other very closely most of the time. On average the mean surface air temperature over the western U.S. mountainous region has up to 3°C cold bias in winter and spring season for CDAS/Reanalysis II data set and about 2°C warm bias can be found in summer for the ERA40 data set. The biases in the eastern U.S. plain are relatively small.

[48] Over the tropical Central America region [70°W – 60°W , 5°S – 0°], both the Reanalysis data sets depart from the observations obviously and sometimes the anomaly signs are even opposite. The annual cycle also does not follow the observation very well. Both the Reanalysis data sets have cold biases and the CDAS/Reanalysis II has relatively larger cold biases. Over the South Asia region [85°E – 95°E , 25°N – 30°N], the temperature anomalies and its annual cycle from ERA40 data set agree with the observation reasonably well. However, at most times the anomalies from the CDAS/Reanalysis II data set are clearly apart from the observation. Its annual cycle closely follows the observation, but with 2° – 3°C cold biases.

[49] Very similar bias patterns but with even larger differences are obtained by using the CDAS/Reanalysis I and ERA40 data sets in comparison to the CRU climatology for the period of 1961–1990, which are also comparable with those results found in the ERA40 Project Report Series [Hagemann *et al.*, 2005]. These results suggest that none of the Reanalysis MMSAT may, as of now, not be suitable as an input forcing for models (such as H96) and model validation in general, even though its anomalies may be suitable for verification over simple terrain in the midlatitudes.

5. Summary

[50] A station observation based global monthly land surface air temperature data set at 0.5×0.5 latitude-

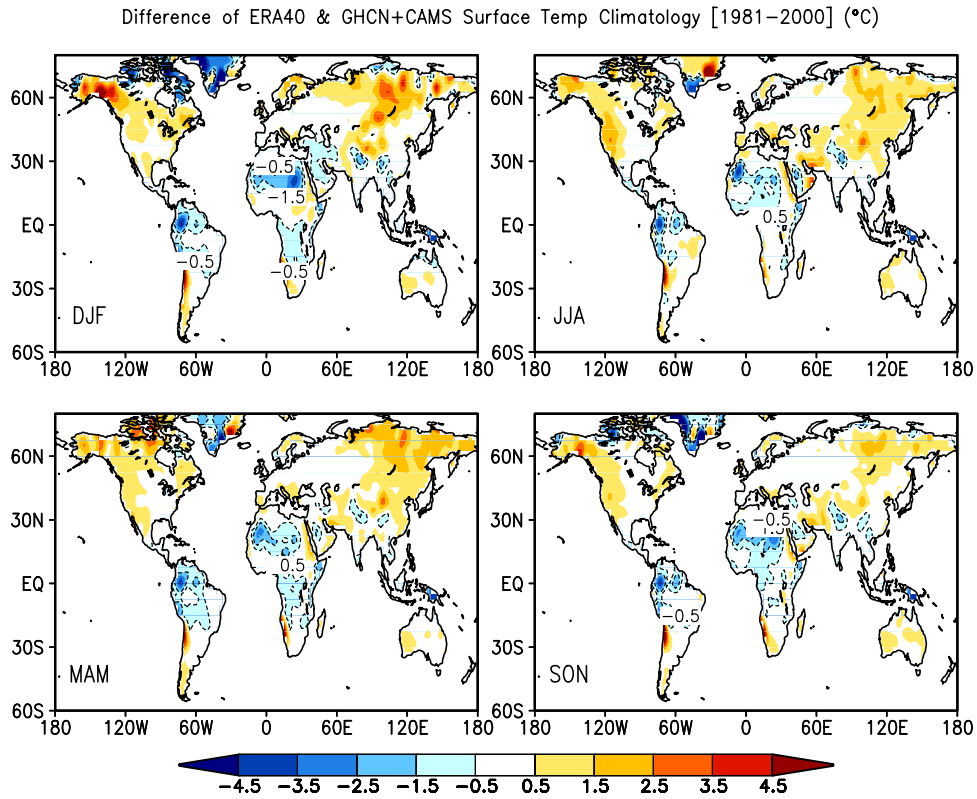


Figure 12. Difference between the seasonal mean (DJF, MAM, JJA, and SON) European Center for Medium-Range Weather Forecasts 40 year Reanalysis (ERA40) climatology and the merged GHCN + CAMS MMSAT climatology (in °C, and negative values are inside the dashed contour) regridded to the ERA40 grid for the period of 1981–2000.

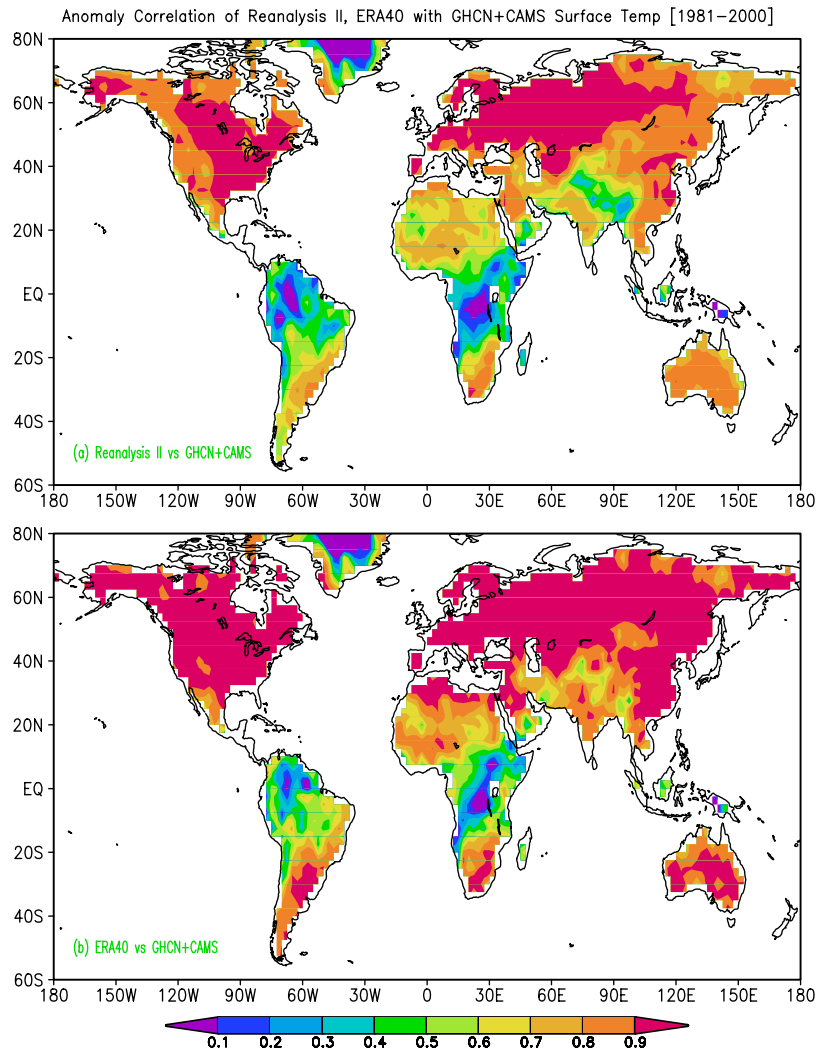


Figure 13. Anomaly correlations between (a) the Reanalysis II and GHCN + CAMS surface air temperature fields and (b) the ERA40 and GHCN + CAMS surface air temperature fields.

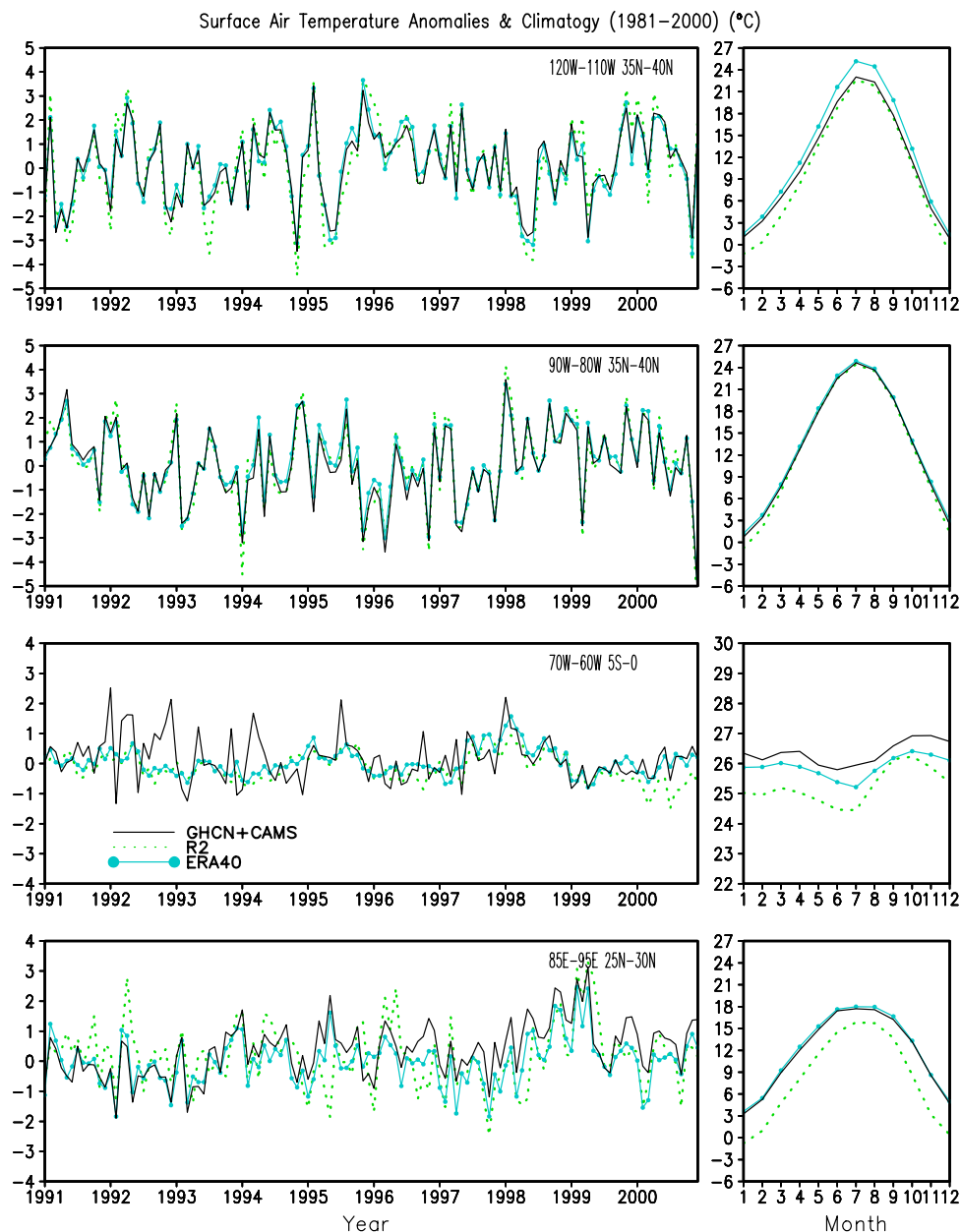


Figure 14. (left) Time series of surface air temperature anomalies and (right) their annual cycles averaged over the selected regions for the period of 1981–2000 from the GHCN + CAMS (solid line), Reanalysis II (dotted line), and ERA40 (closed circle) data sets. The averaging domains are shown in each figure and named as the western U.S. mountainous region, the eastern U.S. plain, the tropical Central America, and the South Asia region, respectively.

longitude resolution for the period of 1948 to present was developed recently at the Climate Prediction Center, National Centers for Environmental Prediction. This data set is different from some existing surface air temperature data sets in (1) using the merged GHCN + CAMS data sets, so it can be regularly updated in near real time with plenty of stations and (2) some unique interpolation methods, such as the anomaly interpolation approach and a spatially and temporally varying temperature lapse rate, derived from the observation based NCEP-DOE Reanalysis II, for topographic adjustment.

[51] The GHCN version 2 data set used here consists of 7280 stations over the globe. It has rich data in the older history but collects new data with some serious time delay. The CAMS data set consists of 6158 stations worldwide and stably collects data from real time based GTS after 1981. There are about 2450 stations in the CAMS data set that in terms of station ID, are duplicates of the GHCN data set. For the remaining nonduplicate 3708 stations, most of them are located outside the United States. The CAMS data set not only brings in about 3700 new stations but also patches many missing data points for duplicate stations in the

GHCN data set. The merged GHCN + CAMS data set has 10978 nonduplicate stations worldwide.

[52] When compared with several existing observation based land surface air temperature data sets, the preliminary results show that the quality of this new GHCN + CAMS land surface air temperature analysis is reasonably good and the new dataset can capture most common temporal-spatial features in the observed climatology and anomaly fields over both regional and global domains.

[53] The study here reveals that there are clear biases between the observed (e.g., the GHCN + CAMS) MMSAT and the existing Reanalysis data sets, such as CDAS/Reanalysis I, II and ERA40 data sets, and these differences vary with season over the global domain. The primary purpose of this work is to generate an observation based global monthly land surface air temperature analysis to replace the previously used 2 m air temperature fields from the NCEP-NCAR global Reanalysis I, which were not observation based. The new global land surface air temperature analysis, together with the CPC global land surface precipitation analysis, will be used to derive other land surface variables, such as the soil moisture, evaporation, runoff, snow accumulation, and snow melt. As a byproduct, this monthly mean surface air temperature data set can also be applied, with caution, to monitor surface air temperature variations over global land routinely or to verify the performance of model simulation and prediction. Interested readers can download the data set from <ftp://ftp.cpc.ncep.noaa.gov/wd5lyf/GHCN-CAMS/>.

[54] **Acknowledgments.** The authors are very grateful to M. Chen and P. Xie for their invaluable discussions, comments, and technical support throughout this study. We thank J. Schemm and J. Janowiak for all their help during the early stage of this work and appreciate P. Xie, M. Halpert, and G. White for internal reviews. We would like to thank C. Ropelewski, C. Daly, and the four anonymous reviewers for insightful comments and suggestions. The ERA40 data set was downloaded from the NCAR Research Data Archive. We also want to thank the CRU group and PRISM group for letting us download and use their climatology dataset. This project was supported by the GAPP grant GC04-039.

References

- Bolstad, P., L. Swift, F. Collins, and J. Regniere (1998), Measured and predicted air temperatures at basin to regional scale in the southern Appalachian mountains, *Agric. For. Meteorol.*, *91*, 161–176.
- Chen, M., P. Xie, J. E. Janowiak, and P. A. Arkin (2002), Global land precipitation: A 50-yr monthly analysis based on gauge observations, *J. Hydrometeorol.*, *3*, 249–266.
- Cressman, G. F. (1959), An operational objective analysis system, *Mon. Weather Rev.*, *87*, 367–374.
- Daly, C. (2006), Guidelines for assessing the suitability of spatial climate data sets, *Int. J. Climatol.*, *26*, 707–721.
- Easterling, D. R., T. C. Peterson, and T. R. Karl (1996), On the development and use of homogenized climate data sets, *J. Clim.*, *9*, 1429–1434.
- Fan, Y., and H. van den Dool (2004), The CPC global monthly soil moisture data set at ½ degree resolution for 1948–present, *J. Geophys. Res.*, *109*, D10102, doi:10.1029/2003JD004345.
- Gandin, L. S. (1965), *Objective Analysis of Meteorological Fields* (in Russian), Gidrometeoizdat, St. Petersburg, Russia. (English translation, 242 pp. Isr. Program for Sci. Transl., Jerusalem.)
- Hagemann, S., K. Arpe, and L. Bengtsson (2005), *Validation of the Hydrological Cycle of ERA-40, ERA-40 Proj. Rep. Ser.*, vol. 24, 42 pp., ECMWF, Reading, U. K.
- Harlow, R. C., E. J. Burke, R. L. Scott, W. J. Shuttleworth, C. M. Brown, and J. R. Petti (2004), Research Note: Derivation of temperature lapse rates in semi-arid south-eastern Arizona, *Hydrol. Earth Syst. Sci.*, *8*(6), 1179–1185.
- Higgins, R. W., W. Shi, E. Yarosh, and J. Schaake (2004), New orographic adjustments improve precipitation analysis For GAPP, *GEWEX News*, *14*, 8–9.
- Huang, J., H. M. van den Dool, and K. G. Georgakakos (1996), Analysis of model-calculated soil moisture over the US (1931–1993) and applications to long range temperature forecasts, *J. Clim.*, *9*, 1350–1362.
- Hulme, M. (1992), 1951–80 global land precipitation climatology for the evaluation of general circulation models, *Clim. Dyn.*, *7*, 57–72.
- Kanamitsu, M., W. Ebisuzaki, J. Woolen, S.-Y. Yang, J. Hnilo, M. Fiorino, and G. Potter (2002), NCEP-DOE AMIP-II Reanalysis (R-2), *Bull. Am. Meteorol. Soc.*, *83*, 1631–1643.
- Kistler, R., et al. (2001), The NCEP-NCAR 50-Year Reanalysis: Monthly means CD-ROM and documentation, *Bull. Am. Meteorol. Soc.*, *82*, 247–268.
- New, M., M. Hulme, and P. Jones (1999), Representing twentieth-century space-time climate variability. Part I: Development of a 1961–90 mean monthly terrestrial climatology, *J. Clim.*, *12*, 829–856.
- Peterson, T., and R. Vose (1997), An overview of the Global Historical Climatology Network temperature data base, *Bull. Am. Meteorol. Soc.*, *78*, 2837–2849.
- Reynolds, R. W., and T. M. Smith (1994), Improved global sea surface temperature analyses using optimal interpolation, *J. Clim.*, *7*, 929–948.
- Rolland, C. (2002), Spatial and seasonal variations of air temperature lapse rates in alpine regions, *J. Clim.*, *16*, 1032–1046.
- Ropelewski, C. F., J. E. Janowiak, and M. S. Halpert (1984), The Climate Anomaly Monitoring System (CAMS), 39 pp., Clim. Anal. Cent., NWS, NOAA, Washington, D. C.
- Ropelewski, C. F., J. E. Janowiak, and M. S. Halpert (1985), The analysis and display of real time surface climate data, *Mon. Weather Rev.*, *113*, 1101–1106.
- Saha, S., et al. (2006), The NCEP climate forecast system, *J. Clim.*, *19*, 3483–3517.
- Uppala, S. M., et al. (2005), The ERA40 Reanalysis, *Q. J. R. Meteorol. Soc.*, *131*, 2981–3012.

Y. Fan and H. van den Dool, Climate Prediction Center, NOAA/National Weather Service, National Centers for Environmental Protection, 5200 Auth Road, Room 806, Camp Springs, MD 20746, USA. (yun.fan@noaa.gov)